Reliability Analysis of Aeroengine Teaching System Based on Virtual Reality Technology

Mingfei Qu(✉) and Xin Zhang

College of Aeronautical Engineering, Beijing Polytechnic, Beijing 100176, China
qmf4528@163.com

Abstract. The emergence of virtual reality technology provides new technological support for the development of teaching, enabling students to immerse themselves more in the teaching environment. However, there is relatively little research on the application of virtual reality technology in aviation engine teaching, which cannot guarantee its reliability. Therefore, a reliability analysis study of aviation engine teaching system based on virtual reality technology is proposed. Select the professional virtual reality modeling and simulation software LabVIEW to construct a three-dimensional model of an aviation engine, design a human-computer interaction teaching process, build a three-dimensional vision model based on the principle of human eye stereo vision, analyze the generation of three-dimensional graphics in the computer, and thus achieve the operation of the aviation engine teaching system. The experimental data shows that under different experimental conditions, the maximum display integrity of the teaching scene obtained after the application of the designed system is 98%, and the maximum success rate of human-machine interaction in the teaching process is 96%, fully confirming the stronger reliability of the designed system.

Keywords: Aeroengine · Reliability · Virtual Reality Technology · 3D Model · Human Machine Interaction

1 Introduction

With the rapid development of information technology, the existing aviation engine teaching mode cannot meet the needs of practical applications. New teaching media are constantly emerging, and after multimedia, a new type of teaching media has emerged in the field of teaching technology, which is virtual reality technology. Traditional aviation engine teaching experiments generally include viewing real engine prototypes in the showroom and conducting engine test runs. However, the internal structure of aviation engines is very complex and difficult to observe, and it is not possible to observe the internal structure solely by observing the actual engine prototype. Moreover, it is difficult to have a comprehensive understanding of the connection relationship between the entire engine and various components. Conducting an aviation engine test drive experiment is not only expensive, but also incurs significant engine losses, making it too expensive

L. Yun et al. (Eds.): ADHIP 2023, LNICST 549, pp. 224–238, 2024.
https://doi.org/10.1007/978-3-031-50549-2_16

to use as a teaching experiment. For students majoring in science and engineering, the practical aspect has become an important aspect for them to deeply understand theoretical knowledge. However, currently, there are problems with outdated equipment and high experimental expenses in aviation engine teaching experiments, making it difficult to meet the practical needs of students in the learning process and keep up with the rapid development of science and technology. Given the above reasons, it is urgent to adopt a new teaching experimental method to ensure a certain level of teaching quality.

Virtual reality technology transforms multimedia teaching platforms from two-dimensional planes to three-dimensional spaces, creating a virtual, realistic, and interactive teaching environment. It can build a three-dimensional virtual space, and students will become a member of this virtual space, and can interact with this space to effectively simulate human behavior in the natural environment, such as seeing, listening, and moving. It is an advanced human-computer interaction technology, which is the intersection and integration of many disciplines, integrating multimedia technology, artificial intelligence, computer graphics, multimedia technology, sensor technology High speed parallel Real-time computing technology and human behavior research and other technologies.

From the existing research results, virtual reality technology is mainly applied in the process of physics teaching, such as fluid real-time simulation systems based on virtual reality technology and physics laboratory teaching systems based on virtual reality technology. However, there are few research achievements related to the application of virtual reality technology in the field of aviation engine teaching.

Therefore, this article applies virtual reality technology to aviation engine teaching and experimentation, proposing a new type of aviation engine teaching and experimentation method, which has important theoretical significance and application value for the digitization and modernization construction of aviation engine teaching and experimentation.

2 Aeroengine Teaching System Design Research

2.1 Aeroengine 3D Modeling Module

According to the performance requirements of the aeroengine teaching system, the professional virtual reality modeling and simulation software LabVIEW is selected to conduct three-dimensional modeling of aeroengines.

The general steps for modeling the solid model aeroengine are:

Step 1: Get modeling data

The internal structure of an aeroengine is very complex, and there are many complicated accessories besides a few main components. The model used in teaching should be as simple as possible to facilitate observers to understand the internal structure of the engine; Moreover, if the amount of model data is very large, it will affect the real-time performance of the system to a certain extent [3]. Therefore, it is necessary to simplify the model. The geometric shape data of the engine model mainly comes from the engineering drawings and photos of the real prototype. Combining with the components we

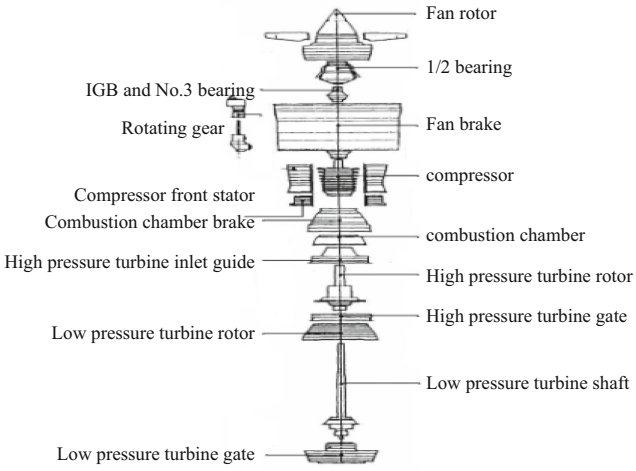

Fig. 1. Schematic Diagram of Aeroengine Structure

care about, we further simplify the engineering drawings to obtain a three-dimensional model of the engine suitable for teaching experiments, as shown in Fig. 1.

There are five main parts of aeroengine: inlet, compressor, combustion chamber, turbine and tail nozzle. We only care about the core engine parts, namely compressor, turbine and combustion chamber, so we omit the inlet port in modeling. Since the tail nozzle will produce tail flame when the engine is working, we need to simulate the effect of tail flame in modular experiments, so we do not omit it, but simplify the original prototype and build a contraction nozzle. The original prototype also has an afterburner, but because the afterburner has a long length and occupies a large space, if the afterburner is not removed, the overall observation effect of the engine model will be affected, so the afterburner is partially removed, and the tail nozzle is directly connected behind the low-pressure turbine support plate. The structure of a real engine is very complex, consisting of thousands of parts. In addition to some important parts, there are many accessories and accessories. The guiding principle of our simplified model is to establish key components that have an important impact on the engine performance, have a great relationship with the shape, and play an important role in rotor rotation, such as blades, disks, casings, flame tubes, shafts, bearings, engine housings, etc. Components such as accessory drive, lubricating oil system, fuel system and control system will be omitted during modeling. When the engine is working, the low-pressure turbine rotor drives the low-pressure compressor to rotate, and the high-pressure turbine rotor drives the high-pressure compressor to rotate. In order to realize the rotation of the engine rotor blade, 7 bearings are built, including 5 roller support bearings and 2 ball bearings.

Step 2: Determine the database hierarchy of the model

3D models are managed and operated in the way of model database. The model database reflects the geometric space position of each entity in the real environment, as well as the structural relationship between models and within models, and determines the hierarchy of all entity models in the virtual scene. Hierarchical division of models

can facilitate the division of modeling and the organization and management of entity models. Hierarchical division of entity models can decompose complex models into several basic units from top to bottom, clarify the objectives of model construction, and greatly reduce the workload of modeling [4]. LabVIEW modeling provides a tree hierarchy structure to organize and manage the model. When modeling, you should first decompose the model according to the hierarchy structure, and arrange the parts at the appropriate node locations for management.

The hierarchy diagram of aeroengine model is shown in Table 1.

Table 1. Aero engine structure hierarchy

Level 1	Level II	Level 3
compressor	High pressure compressor	Rotor blade
		stator vane
		Wheel disc
	Low pressure compressor	–
turbine	Turbine guide vane	–
	High pressure turbine	–
	Low pressure turbine	–
combustion chamber	Cross flame tube	–
	Flame tube	Flame tube wall
	Combustion chamber shell	–
	Lower wall of expander gate	–
Machine brake	External brake	Low pressure compressor brake
		Outer channel housing
	Internal machine brake	High pressure compressor brake
		Turbine gate
axis	axis	Inner shaft
		Outer shaft
	Bearing	Low pressure bearing
		High pressure bearing
	Head fairing	–
	Nozzle tailstock	–

Step 3: Establish the model

According to the hierarchical structure and drawings planned in advance, establish a 3D model [5] in LabVIEW. When modeling, the complexity of internal parts of the engine is taken into consideration, and the modeling is carried out according to the size scale of 10:1 (model size: real size). The full model of aeroengine is shown in Fig. 2

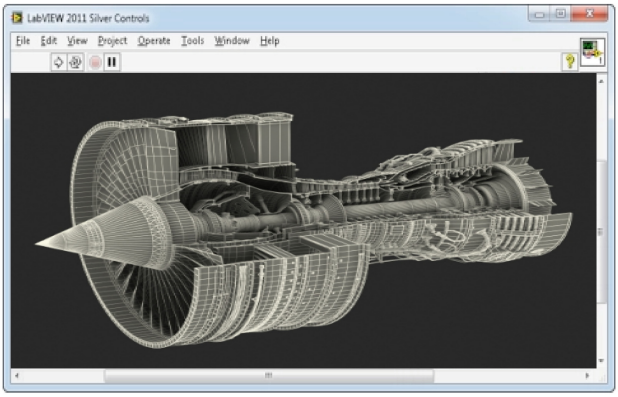

Fig. 2. Schematic Diagram of Aeroengine Full Model

As shown in Fig. 2, the components of 3D visual simulation model are as follows:

Low pressure compressor: 5-stage axial flow type. The rotor adopts a drum disk structure, and the rotor adopts two roller bearing;

High pressure compressor: 12 stage axial flow type. The rotor adopts a drum disk structure, the inlet is provided with an inlet guide vane, and the rotor adopts a roller bearing and a ball bearing;

Combustion chamber: annular tube type reflux combustion chamber. There are 8 flame tubes, 8 fuel nozzles, 2 igniters and 8 cross flame tubes;

High pressure turbine: two-stage axial flow type. There is a roller bearing at the front end;

Low pressure turbine: two-stage axial flow type. There is a roller bearing at the rear end;

Shaft: double shaft rotor;

Outer casing: LP compressor casing, HP compressor casing, diffuser casing, combustion chamber casing, turbine guide casing.

The above process completed the construction of the three-dimensional model of the aeroengine, which laid a solid foundation for the follow-up research.

2.2 Human Computer Interaction Module in Teaching Process

Human computer interaction is the key to the realization of aeroengine teaching process. Its main application technology is virtual hand technology, which mainly uses computers to create a virtual environment, and makes the virtual hand model as the replacement of human hands in the virtual environment. The operator transmits the operation information of human hands to the virtual hand model in the virtual scene through virtual peripherals (data gloves). Realize the action mapping from human hand to virtual hand, and get information feedback (force/tactile feedback) from the virtual environment, so as to achieve interaction with the virtual environment. Virtual hand technology is a new technology with multi - discipline. It involves gesture input technology, position tracking technology, virtual hand modeling technology, stable grasping technology, etc.

Virtual hand models can be presented to users in a visual manner, enabling them to intuitively understand the position, posture, and movements of the hand. This helps to improve users' understanding of system operations and interaction processes, and promotes effective communication with computer systems. Through the virtual hand model, users can operate and interact with their hands in a natural way in the virtual environment. This simulation experience can enhance users' perception and control of operations, providing a more realistic interaction experience. Virtual hand technology is the key to realize the engine virtual assembly in this teaching simulation system [6].

For human-computer interaction based on virtual hand, it is to use data gloves to measure the angle of each joint on the human hand, use position trackers to measure the spatial position of the human hand, control the motion and state of the virtual hand model in the computer according to the measured motion data, and use virtual hands to grasp, release, and translate virtual objects. And calculate the position and attitude of the moved virtual object. Finally, the operator judges whether to complete the operation according to various sensory feedback, and then starts a new task. Human computer interaction based on virtual hand consists of operator, virtual peripheral and virtual environment, as shown in Fig. 3.

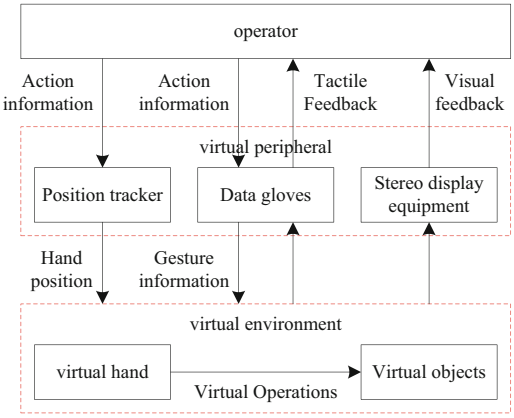

Fig. 3. Schematic diagram of human-computer interaction framework in the teaching process based on virtual hands

Among them, gesture input technology is one of the key technologies of virtual hand technology. At present, there are many methods of gesture recognition, mainly including gesture input based on data gloves and gesture input based on computer vision. This paper mainly applies gesture input technology based on data glove. This technology uses data gloves as an interactive tool for gesture input. The data glove used in this system is 5DT Data Glove 5 produced by 5DT Company. The 5DT Data Glove 5 data glove is a black elastic double-layer textile. The interlayer is a leather sensor made of optical fibers. There is a sensor on each finger to measure the average flexion and extension of the finger (that is, the flexion and extension of the joint in the middle of the finger). There are also two sensors at the wrist to measure the pitch angle and tilt angle of the palm. The position distribution of sensors is shown in Fig. 4.

Fig. 4. 5DT Data Glove Sensor Distribution Diagram

5DT Data Glove 5 has working modes such as command, report data, continuous data, and analog mouse. The sampling rate of the data glove can be up to 200 Hz. The data string sampled from the glove has a total of 9 bytes, and the specific meaning is shown in Table 2.

Table 2. Meaning of Data String Bytes Collected by Data Gloves

Byte sort	byte	meaning
1	Header	The leading byte indicates the beginning of a new data string
2	F1	Flexion and extension of thumb
3	F2	Flexion and extension of index finger
4	F3	Flexion and extension of middle finger
5	F4	Flexion and extension of ring finger
6	F5	Flexion and extension of little finger
7	pitch	Tilt angle of hand swing up and down
8	roll	Tilt angle of palm rotation
9	checksum	Checksum

Since the data glove has no position sensor, the position information of the hand in the three-dimensional space cannot be obtained from the input data of the data glove. Therefore, in this application system, the position change of the hand in the three-dimensional space is not obtained through the data glove, but through the position tracker.

In order to better control the state of the virtual hand grasping the virtual object, we add the grasping state flag bit to the virtual object. True indicates that the virtual hand has

grasped the object, and false indicates that the virtual hand has not grasped the object; We set the initial value of the grab status flag bits of all virtual objects in the scene to false. The position, orientation and posture of the virtual hand are obtained by acquiring the spatial position and orientation of the human hand and the angle values of each joint from the SDT data glove and FOB electromagnetic tracker; Then, collision detection is carried out to determine the grabbing status of virtual objects according to the grabbing rules, set the grabbing status flag bit of virtual objects in combination with the current grabbing status, and correspondingly realize the grabbing or releasing of virtual objects [7].

The algorithm flow of the whole virtual hand grabbing virtual objects is shown in Fig. 5.

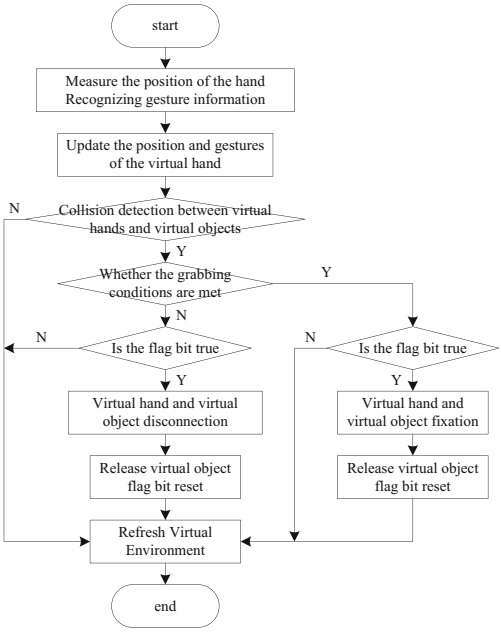

Fig. 5. Flow Chart of Virtual Hand Grasping Virtual Objects

As shown in Fig. 5, the detailed steps of the virtual hand grasping algorithm are as follows:

Step 1: execute actions according to assembly requirements; Obtain the value of the electromagnetic tracker, that is, the absolute spatial position and orientation value of the hand, obtain the value of each sensor of the data glove, and convert it into the corner value of each joint of the finger.

Step 2: The computer calculates the parameters required for the motion of the virtual hand according to the obtained spatial position and orientation values of the human hand, as well as the rotation angles of the finger joints, and updates the position and gesture of the virtual hand in the virtual operation space according to these parameters.

Step 3: Collision detection between virtual hand and virtual object. If there is no collision between the two, go to step 6; If there is a collision between the two, judge whether the virtual hand and the virtual object meet the snatch conditions [8].
Step 4: if the snatch conditions are met, judge the marking position. If it is true, the coordinate system of the virtual hand is fixed with the coordinate system of the virtual object, the virtual object is grabbed by the virtual hand, and the virtual object pair is translated and rotated with the virtual hand. Mark position 1, and turn to step 6; Otherwise, go to step 6 directly.
Step 5: if the conditions for snatch are not met, judge the mark position. If it is true, remove the connection between the virtual hand and the virtual coordinate system, release the virtual object with the virtual hand, mark position 0, and turn to step 6; Otherwise, go to step 6 directly.
Step 6: Refresh (redraw) the virtual environment and turn to step 1.
The above process details the whole process of teaching human-computer interaction, which provides support for aeroengine teaching experiments.

2.3 Teaching Scene Stereoscopic Display Module

In virtual reality, stereoscopic display technology is one of the key technologies. It is a necessary condition for a virtual reality based system. Without in-depth stereoscopic visual effects, it is impossible to feel immersive, and it is also impossible to achieve the goal of virtual reality. In order to generate stereoscopic images and enable users to see high-quality stereoscopic effects, we need to conduct in-depth research on the hardware implementation and software algorithm of stereoscopic display. This section focuses on introducing the principle of human eye stereoscopic vision, so as to propose a stereoscopic vision model, then analyze the generation of three-dimensional graphics in the computer, and finally give an example of stereoscopic effects.

Because people's eyes are a certain distance apart, the image of the same object in the left and right eyes will be slightly different, and this difference will form the main clue to judge the depth information of the static scene. Binocular parallax is actually the angle difference caused by the binocular imaging of two objects with a certain distance in the depth direction in space, and the calculation formula is

$$\delta = 2\left(\arctan\frac{L}{2D} - \arctan\frac{L}{2(D+\Delta D)}\right) \tag{1}$$

In formula (1), δ it represents an object O_1 and O_2 poor perspective; L is the distance between pupils; D it indicates the distance between the object and the eye.

When D much greater than L Eq. (1) can be written as:

$$\delta \approx \frac{L}{D} - \frac{L}{D+\Delta D} = \frac{L\Delta D}{D(D+\Delta D)} \tag{2}$$

If the object O_1 object O_2 be relative to O_1 the depth position of δ the size of the corner. In fact, the human eye cannot directly feel δ. However, the vision system can get the information of depth direction by comparing the position difference of the object imaging on the retina. Binocular parallax is only effective in a small range in depth

perception, which is generally considered to be 0–100. When the visual distance of an object is less than 380mm, that is, when the angle of the object to both eyes is less than a certain value, diplopia will occur, and the stereoscopic feeling cannot be formed. This effect must be taken into account in the design of stereoscopic display to avoid the stereoscopic image pair being difficult to fuse and thus unable to produce stereoscopic sense [9].

Three algorithms are usually used to generate three-dimensional images in vision systems: left and right eye view generation based on projection transformation principle; Stereogram generation algorithm based on correlation theory; Fast holographic imaging algorithm. The algorithm based on correlation theory is an improvement of the algorithm based on projection transformation, and their basic principles are the same; Fast hologram generation algorithm is the only image generation technology that can provide all depth clues. It has high computing efficiency, but requires special hologram imaging equipment. The principle of left and right eye view generation algorithm based on projection transformation principle is briefly described below.

a. Single view perspective projection

Single viewpoint perspective is a single vanishing point perspective, which takes the viewpoint as the projection center, and the line of sight starts from the viewpoint. Unlike parallel projection, the line of sight is not parallel. The line of sight crosses the projection plane and intersects the object. The intersection point with the projection plane is the corresponding image point of the intersection point of the line of sight and the object. The viewpoint of perspective projection is $P_c(x_c, y_c, z_c)$, the projection plane is XOY plane, a point on the body $P(x, y, z)$ the projection of is $P_s(x_s, y_s, z_s)$, the expression is

$$\begin{cases} x_s = x_c + (x - x_c) \times t \\ y_s = y_c + (y - y_c) \times t \\ z_s = z_c + (z - z_c) \times t \end{cases} \tag{3}$$

In Eq. (3), t it refers to auxiliary calculation parameters, which are calculated by the following formula:

$$t = -\frac{z_c}{z - z_c} \tag{4}$$

Substitute Formula (4) into Formula (3) to get the projection line equation, which is expressed as

$$\begin{cases} x_s = \frac{x_c - xz_c}{z - z_c} \\ y_s = \frac{y_c - yz_c}{z - z_c} \end{cases} \tag{5}$$

To facilitate the research, set the perspective projection viewpoint at Z negative half axis, the distance from the origin is d, there are: $x_c = y_c = 0$, $z_c = -d$, and substitute it into formula (5) to obtain the final projection line equation, which is expressed as

$$\begin{cases} x_s = \frac{xd}{z+d} \\ y_s = \frac{yd}{z+d} \end{cases} \tag{6}$$

b. Double viewpoint projection of left and right eyes

For stereoscopic images, it is required to generate different views relative to the left and right eyes. Each eye observes the scene from different positions, so that two eyes can see different pictures. These views are generated according to different projection centers [10]. Set the coordinate system OXYZ as the world coordinate system, the projection plane is located at $Z = 0$, and the distance between two eyes is e, the projection center corresponding to the left view is $L\left(-\frac{e}{2}, 0, -d\right)$, the projection center of the right view is $R\left(\frac{e}{2}, 0, -d\right)$, d Is the distance from the viewpoint to the projection plane.

Spot $P(x, y, z)$ taking the left viewpoint as the projection center, the expression of the projection point generated by projection onto the XOY plane is

$$\begin{cases} x_{sL} = \frac{xd - ze/2}{z+d} \\ y_{sL} = \frac{yd}{z+d} \end{cases} \tag{7}$$

In Eq. (7), (x_{sL}, y_{sL}) it represents a point $P(x, y, z)$ the projection point generated by taking the left viewpoint as the projection center and projecting it onto the XOY plane [11].

Same $P(x, y, z)$ the point takes the right viewpoint as the projection center, and the expression of the projection point on the XOY plane is

$$\begin{cases} x_{sR} = \frac{xd + ze/2}{z+d} \\ y_{sR} = \frac{yd}{z+d} \end{cases} \tag{8}$$

In Eq. (8), (x_{sR}, y_{sR}) it represents a point $P(x, y, z)$ the projection point generated by taking the right viewpoint as the projection center and projecting it onto the XOY plane.

When the projection map is displayed on the CRT screen, the coordinates of the projection point on the XOY plane need to be converted to the local viewport coordinate system [12]. The coordinate axes of the left and right viewport coordinate systems are parallel to the world coordinate system respectively, and the left viewport coordinate system moves left along the X axis from the world coordinate system $\frac{e}{2}$ the right viewport coordinate system is moved right along the X axis from the world coordinate system $\frac{e}{2}$ get. Thus, it is obtained that $P(x, y, z)$ the coordinates of the left image point in the left viewport coordinate system are $\left(x'_{sL}, y'_{sL}\right)$, $P(x, y, z)$ the coordinates of the right image point in the right viewport coordinate system are $\left(x'_{sR}, y'_{sR}\right)$. Only the projection points in the left and right viewports are displayed on the screen, and the contents in the whole left and right viewports will be displayed in the same area of the screen. At this time, the formula for calculating the relative distance between the two image points is

$$S = x'_{sL} - x'_{sR} = e\left(1 - \frac{z}{z+d}\right) \tag{9}$$

So, point $P(x, y, z)$ the image in the left and right eyes has a certain sense of distance S, form parallax, and form stereoscopic sense through brain fusion. S the size of, which affects the quality of image fusion, depends on the distance between two viewpoints and the relative position of the object, projection center, and projection plane [13]. In

practical applications, the size of the final screen display area should also be considered. It is one of the key tasks of the stereoscopic display system to select the projection center spacing according to the different sizes of the screen display area, so as to form a better image fusion effect.

Through the design and development of the above three modules, the operation of the aeroengine teaching system is realized, which provides effective support for the aeroengine experiment teaching.

3 Design System Reliability Analysis

3.1 Selection of Virtual Instrument

In the virtual instrument system, hardware is only for signal acquisition, and software is the key of the whole instrument. When the user's test requirements change, or the test items need to be added or reduced, the user only needs to change the software program appropriately to get the test instrument system that meets the test requirements. This is the meaning of the slogan "The Software Is The Instruments" put forward by National Instruments, the initiator of virtual instruments. The software provides three main functions: an integrated development environment, an advanced interface with the instrument hardware, and a graphical user interface. The main software modules include data acquisition, data analysis, data display, file management and report output. The main development environments of virtual instruments include C, C++ Builder, VB, Delphi, LabVIEW, LabWindows/CVI, etc. LabVIEW, which is a fully graphical special development tool for virtual instruments, integrates a large number of instrument function modules internally. The development environment based on graphical programming language G enables developers to focus only on instrument functions and liberate themselves from complex, tedious and time-consuming language programming. Compared with the traditional programming method, using LabVIEW to design virtual instruments can improve the efficiency by 4–10 times.

The design steps of LabVIEW are shown in Fig. 6.

The virtual instruments selected above are used as experimental equipment to facilitate the subsequent experiments.

3.2 Analysis of Experimental Results

In order to intuitively display the reliability of the design system, the fluid real-time simulation system based on virtual reality technology and the physical laboratory teaching system based on virtual reality technology are selected as comparison systems 1 and 2, and the integrity of teaching scene display and the success rate of human-computer interaction in the teaching process are set as the evaluation indicators of system reliability. The calculation formula is

$$\begin{cases} Q = \frac{q_1}{q_{tptal}} \times 100\% \\ K = \frac{k_1}{k_{total}} \times 100\% \end{cases} \tag{10}$$

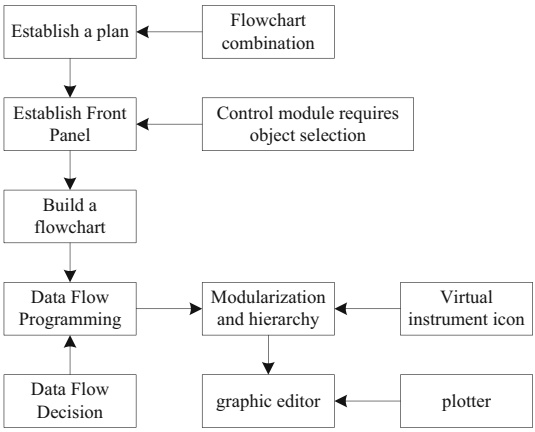

Fig. 6. Schematic diagram of LabVIEW design steps

In Eq. (10), Q it represents the display integrity of teaching scenes; K it represents the success rate of human-computer interaction in the teaching process; q_1 it represents the display area of the teaching scene; q_{total} it represents the total area displayed in the teaching scene; k_1 it indicates the number of successful human-computer interaction in the teaching process; k_{total} it represents the total number of human-computer interactions in the teaching process.

The display integrity of teaching scenes obtained through experiments is shown in Fig. 7.

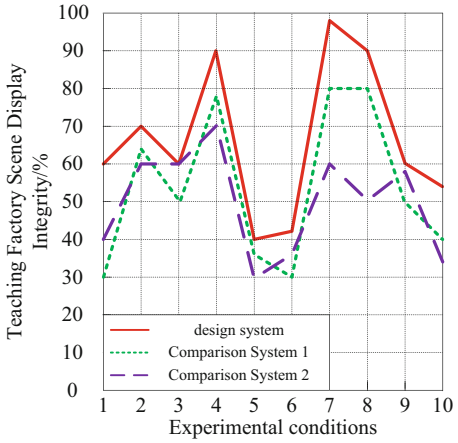

Fig. 7. Schematic Diagram of Teaching Scene Display Integrity

As shown in the data in Fig. 7, under different experimental conditions, the completeness of the teaching scene display was obtained by comparing System 1 with 30%–80%, and by comparing System 2 with 30%–70%. However, after the design and application of

the system, the completeness of the teaching scene display was obtained by 40%–98%. The completeness of the teaching scene display was much higher than that of Comparing System 1 and System 2, providing more complete teaching scene support for aviation engine teaching.

The success rate of human-computer interaction in the teaching process obtained through experiments is shown in Table 3.

Table 3. Data sheet of human-computer interaction success rate in teaching process/%

Test conditions	design system	Comparison system 1	Comparison system 2
1	89	56	45
2	94	45	44
3	95	64	41
4	96	52	56
5	91	58	54
6	80	63	57
7	84	62	50
8	95	64	41
9	91	51	42
10	90	49	38

As shown in Table 3, under different experimental conditions, the success rate of human-machine interaction in the teaching process obtained by comparing System 1 is 45%–64%, and the success rate of human-machine interaction in the teaching process obtained by Comparing System 2 is 38%–57%. However, the success rate of human-machine interaction in the teaching process obtained by designing the system application is 80%–96%. The success rate of human-machine interaction in the teaching process is much higher than that of Comparing System 1 and Comparing System 2, indicating that the success rate of the method in this paper is relatively high, It can provide more stable performance support for aviation engine teaching.

4 Conclusion

Virtual reality technology has become the fastest developing multidisciplinary comprehensive technology in the field of computer science. This technology can provide new technical support for teaching development. However, the application research of this technology in aviation engine teaching is relatively limited, and its reliability cannot be guaranteed. Therefore, a reliability analysis study of aviation engine teaching systems based on virtual reality technology is proposed. By combining aviation engine teaching and experimentation with virtual reality technology, a visual simulation system for aviation engine teaching and experimentation with high real-time, high interactivity, and

deep immersion is designed, which intuitively displays the entire process of the engine during operation. And through experiments, it has been verified that the design system can greatly improve the completeness of teaching scene display and the success rate of human-machine interaction in the teaching process, providing more effective system support for aviation generator teaching.

Acknowledgement. School level project of Beijing Polytechnic, Project Name: Application of virtual reality technology in aeroengine teaching (2022X007-SXZ).

References

1. Qin, T., Cook, M., Courtney, M.: Exploring chemistry with wireless, PC-less portable virtual reality laboratories. J. Chem. Educ. **98**(2), 521–529 (2021)
2. Bu, X., Ng, P., Chen, Q., et al.: Effectiveness of virtual reality-based interventions in rehabilitation management of breast cancer survivors: protocol of a systematic review and meta-analysis. BMJ Open **12**(2), e053745–e053745 (2022)
3. Wang, Y., Chang, F., Wu, Y., et al.: Multi-Kinects fusion for full-body tracking in virtual reality-aided assembly simulation. Int. J. Distrib. Sens. Netw. **18**(5), 625–636 (2022)
4. Schleuinger, M.: Information retrieval interfaces in virtual reality-a scoping review focused on current generation technology. PLoS ONE **16**(2), e0246398–e0246398 (2021)
5. Chen, S.C.: Multimedia in virtual reality and augmented reality. IEEE Multimedia **28**(2), 5–7 (2021)
6. Karsenty, K., Tartakovsky, L., Sher, E.: A diesel engine with a catalytic piston surface to propel small aircraft at high altitudes—a theoretical study. Energies **14**(7), 1905 (2021)
7. Martin, C., Quinn, D., Murphy, A., et al.: Understanding influence of powerplant component connection strategies on aircraft engine structural deformations. J. Aircr. **58**(5), 1–11 (2021)
8. Pang, S., Jafari, S., Nikolaidis, T., et al.: A novel model-based multivariable framework for aircraft gas turbine engine limit protection control. Chin. J. Aeronaut. **34**(12), 57–72 (2021)
9. Zhang, Y.: Interactive intelligent teaching and automatic composition scoring system based on linear regression machine learning algorithm. J. Intell. Fuzzy Syst. **40**(2), 2069–2081 (2021)
10. Robust, An, Z., Li, T.: Simulation of dynamic response of solid rocket engine under standard transportation conditions. Comput. Simul. **39**(10), 66–70 (2022)
11. Xia, Q.: Application of 3Ds max and virtual reality technology in 3D submarine scene modeling. Microprocess. Microsyst. **80**, 103562.1–103562.6 (2020)
12. Song, J., Jiang, L., Wang, L.: P-3.10: current status and prospects of simulation training equipment based on virtual reality and augmented reality technology. In: SID Symposium Digest of Technical Papers, vol. 52, no. 8, pp. 742–745 (2021)
13. Brown, C., Hicks, J., Rinaudo, C.H., et al.: The use of augmented reality and virtual reality in ergonomic applications for education, aviation, and maintenance. Ergon. Des. Q. Hum. Factors Appl. (6), 106480462110034 (2021)